The *Herschel* Planetary Nebula Survey (HerPlaNS): A Comprehensive Dusty Photoionization Model of NGC6781

Masaaki Otsuka,[1] Toshiya Ueta,[2] and HerPLaNS consortium

[1]*ASIAA, 11F of Astronomy-Mathematics Building, AS/NTU. No.1, Sec. 4, Roosevelt Rd, Taipei 10617, Taiwan, R.O.C.*
[2]*Department of Physics and Astronomy, University of Denver, 2112 E. Wesley Ave., Denver, CO 80210, USA*

ABSTRACT

As one of the follow-up studies of the *Herschel* Planetary Nebula Survey (HerPlaNS; Ueta et al. 2014), we focus on a C-rich bipolar planetary nebula (PN) NGC6781 to characterize the dusty nebula and the central star based on our own *Herschel* data and the rich archival spectroscopic/photometric imaging data in wavelengths from UV to radio wavelength. With Cloudy, we construct a comprehensive photoionization model of NGC6781 ever made incorporating data from UV to radio. We reproduce the observed spectral energy distribution (SED) and all the atomic gas, H_2, CO, and OH molecular line fluxes. We estimate the total gas mass to be 0.41 $M_\odot$ by our Cloudy modeling. A significant fraction of this total mass (about 70 %) is found to exist in the photodissociation region (PDR), demonstrating the critical importance of the PDR in PNe that are generally recognized as the hallmark of ionized/H^+ regions. From our detailed multiwavelength analysis of NGC6781, we emphasise that characterizing PDRs and estimating warm-cold gas/dust masses in any astronomical objects would be very important for fully understanding stellar evolution and material recycling in galaxies. Dataset provided by Far-IR *AKARI* and *Herschel* have a critical role to investigate PDRs in PNe.

Keywords: infrared: ISM, ISM: abundances, dust, molecules, planetary nebulae: individual (NGC6781)

RESULTS

We perform a comprehensive analysis of the PN NGC6781 in order to investigate the physical conditions of each of the ionized, atomic, and molecular gas components as well as the dust component in the nebula and the evolution of the

Table 1. The log of panchromatic observations of NGC6781 adopted for the present study.

			Photometry Observations		
Obs-Date	Telescope	Instrument	Band	Program-ID/PI	References
2011-07-25	*GALEX*	GALEX	NUV		
2008-07-31	ING/INT 2.5-m	WFC	RGO U, Sloan g and r	I08AN02/P. Groot	
2015-05-12	ESO/NTT 3.6-m	EFOSC2	Bessel B, V, R	60.A-9700(D)/Calibration	
2009-08-09	ING/INT 2.5-m	WFC	IPHAS Hα	C129/J. Casare	
1995-07-24	*HST*	WFPC2/PC	F555W, F814W (central star only)	GO6119/H.E. Bond	
2010-06-26	UKIRT 3.8-m	WFCAM	J, H, K		
2010-04-13	*WISE*	WISE	3.4, 11.6, 22.1 μm		
2004-04-20	*Spitzer*	IRAC	4.5, 5.8, 8.0 μm	68/G. Fazio	
1996-04-28	*ISO*	ISOCAM	14.3 μm	COX 1/P. Cox	
2011-10-17	*Herschel*	PACS	70, 100, 160 μm	OT1-tueta-2/T. Ueta	(1)
2011-10-11	*Herschel*	SPIRE	250, 350, 500 μm	OT1-tueta-2/T. Ueta	(1)
	Radio telescopes	Various	1.4, 5, 22, 30, 43 GHz		(2), (3), (4), (5), (6)
			Spectroscopy Observations		
Obs-Date	Telescope	Instrument	Wavelength	Program-ID/PI	References
1997-08-09	ING/WHT 4.2-m	ISIS	3600–8010 Å	W-97B-41/X.-W. Liu	(7), (8)
2005-10-19	*Spitzer*	IRS	5.2–39.9 μm	1425/IRS-Calibration	
2011-10-14	*Herschel*	PACS	51–220 μm	OT1-tueta-2/T. Ueta	(1)
2012-04-01	*Herschel*	SPIRE	194–672 μm	OT1-tueta-2/T. Ueta	(1)

References—(1) Ueta et al. (2014); (2) Condon et al. (1998, 376.5 ± 12 mJy at 1.4 GHz); (3) Stanghellini & Haywood (2010, 323 mJy at 5 GHz); (4) Petrov et al. (2007, 190 mJy at 22 GHz); (5) Pazderska et al. (2009, 264.1 ± 7.1 mJy at 30 GHz); (6) Umana et al. (2008, 710 mJy at 43 GHz); (7) Liu et al. (2004a); (8) Liu et al. (2004b).

Corresponding author: Masaaki Otsuka
otsuka@asiaa.sinica.edu.tw

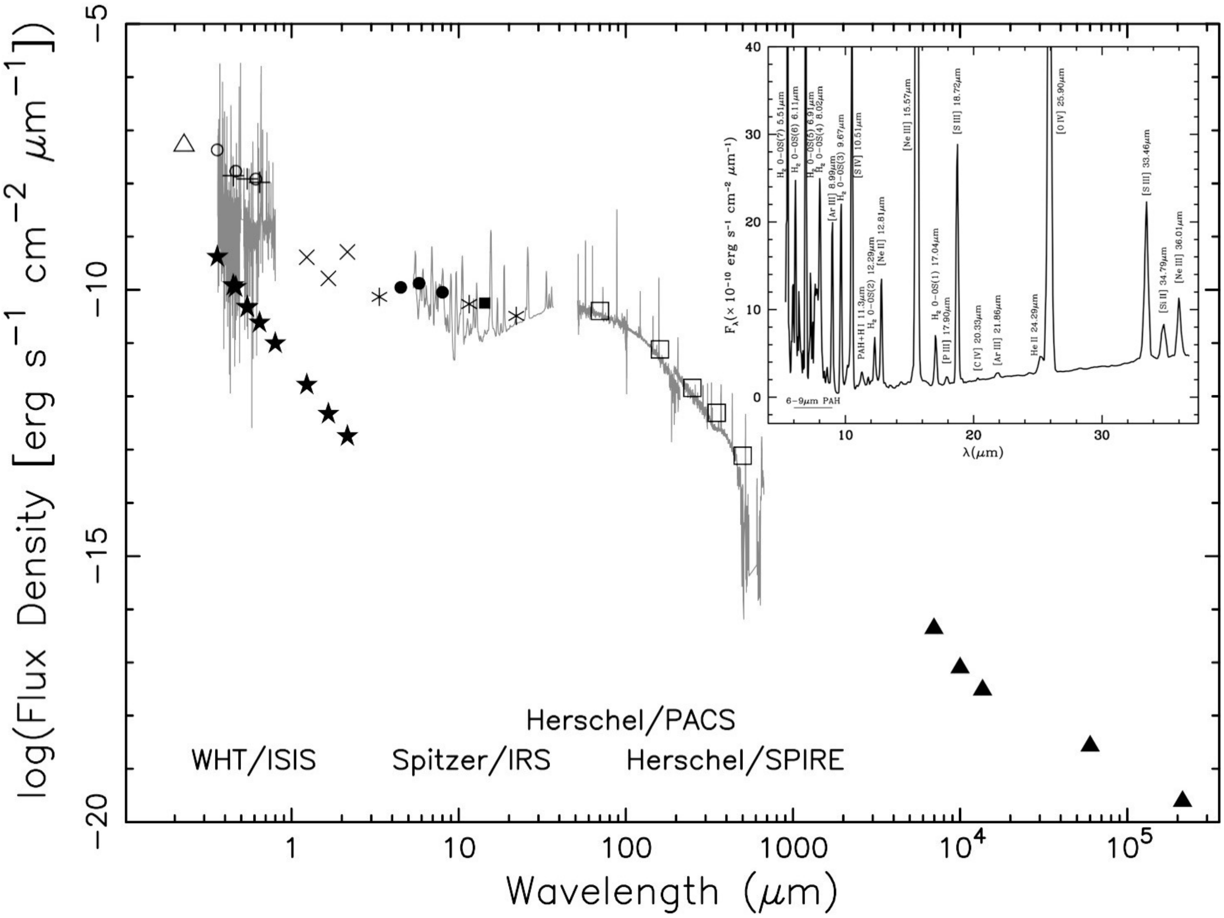

Figure 1. The panchromatic photometric and spectroscopic data of NGC6781 adopted in the present study. Broadband photometry was done over the entire extent of the nebula from the following sources: *GALEX* (open triangle), ING/INT (open circles), ESO/NTT (pluses), UKIRT (crosses), *WISE* (asterisks), *Spitzer* (filled circles), *ISO* (filled square), *Herschel* (open squares), and Radio (filled triangles), while photometry of the CSPN (filled stars) was also done using *HST*/WFPC2 images in addition to the above optical and near-infrared *JHK* sources. Spectra (grey lines) were sourced from WHT/ISIS, *Spitzer*/IRS, and *Herschel*/PACS and SPIRE. The adopted spectra from four instruments are shown in grey lines, with their respective spectral ranges indicated at the bottom. The inset displays the *Spitzer*/IRS spectra in the mid-IR full of H_2, polycyclic aromatic hydrocarbons (PAHs) and ionized gas emission features/lines with the dust continuum steadily rising toward longer wavelengths from around 10 μm. This figure is taken from Otsuka et al. (2017).

central star, based on our own far-IR *Herschel* data (Ueta et al. 2014) and the rich archival spectroscopic/photometric data in the UV to radio wavelength ranges (Figure 1 and Table 1).

Spitzer/IRS mid-IR spectrum covers the polycyclic aromatic hydrocarbon (PAH) 6–9 μm and 11.3 μm bands and pure rotational hydrogen molecule (H_2) lines (Figure 1). The excitation curve plots for the H_2 lines can be fitted by two temperature components with 1161 ± 72 K and 236 ± 50 K. We derived a column density $N(H_2) = (2.72 \pm 0.53) \times 10^{18}$ cm^{-2} and $(6.67 \pm 4.89) \times 10^{19}$ cm^{-2} for the hotter and warm temperature components, respectively. Comparisons of the observed H_2 line intensities relative to the H_2 $v = 0-0$ S(2) at 9.67 μm line with the theoretical shock models by Flower & Pineau Des Forêts (2010) suggest that the H_2 lines are excited by shock interaction with the remnant asymptotic giant branch (AGB) circumstellar envelope.

We perform detailed plasma diagnostics and derived nebular abundances of nine elements He/C/N/O/Ne/Si/S/Cl/Ar (Table 2). By comparing with the AGB nucleosynthesis model of Karakas (2010), we find that the progenitor would be a 2.25–3.0 $M_\odot$ star. The current evolutional status and nebular elemental abundances of the H_2-rich bipolar PN NGC6720 (Ring Nebula) (e.g., van Hoof et al. 2010) are in excellent agreement with NGC6781, suggesting that both PNe have originated from progenitor stars with similar masses and shared similar evolutionary paths.

We construct the photoionization model with Cloudy (Ferland et al. 2013) to be self-consistent with all the observations (Figures 2 and 3). We derive the best-fit distance of 0.46 kpc by fitting the stellar luminosity (as a function of the distance and effective temperature of the central star) with the adopted post-AGB evolutionary tracks. About 70 % of the total dust mass 1.53×10^{-3} $M_\odot$ would be from warm-cold dust components. The derived gas mass of 0.41 $M_\odot$ (0.09 $M_\odot$ ionized atomic gas, 0.20 $M_\odot$ neutral atomic gas, 0.11 $M_\odot$ ionized/neutral molecular gas) corresponds to roughly 60 % of the amount of mass theoretically predicted to have been ejected during the last thermal pulse episode in initially 2.5 $M_\odot$ stars predicted by Karakas (2010). We find that only 20 % of the total gas mass appears to be contained within the ionized

Table 2. Elemental abundances ϵ(X) of NGC6781 derived in the present analysis, compared with the solar abundances (column 3; [X/H] = ϵ(X) − $\epsilon_{\odot}$(X), where $\epsilon_{\odot}$(X) is taken from Lodders 2010), previous empirical analysis (column 4; by Liu et al. 2004a), and model predictions for initially 2.25 and 3.0 $M_{\odot}$ stars with Z = 0.02 (columns 5 and 6, respectively; by Karakas 2010). The number density ratio relative to hydrogen is $\epsilon(X) = \log_{10}(X/H) + 12$, where $\log_{10}(H) = 12$.

X (1)	ϵ(X) (2)	[X/H] (3)	ϵ(X) (4)	ϵ(X) (5)	ϵ(X) (6)
He	11.06 ± 0.17	+0.13 ± 0.17	11.08	11.05	11.06
C	8.56 – 9.00	+0.17 – 0.61	9.17	8.52	9.06
N	8.15 ± 0.09	+0.29 ± 0.15	8.38	8.39	8.42
O	8.76 ± 0.04	+0.03 ± 0.08	8.65	8.94	8.94
Ne	8.15 ± 0.05	+0.10 ± 0.11	8.22	8.12	8.27
Si	7.03 ± 0.27	−0.50 ± 0.28	···	7.57	7.59
S	6.91 ± 0.06	−0.25 ± 0.06	6.97	7.42	7.44
Cl	5.16 ± 0.42	−0.09 ± 0.42	5.43	···	···
Ar	6.49 ± 0.10	−0.01 ± 0.14	6.35	···	···

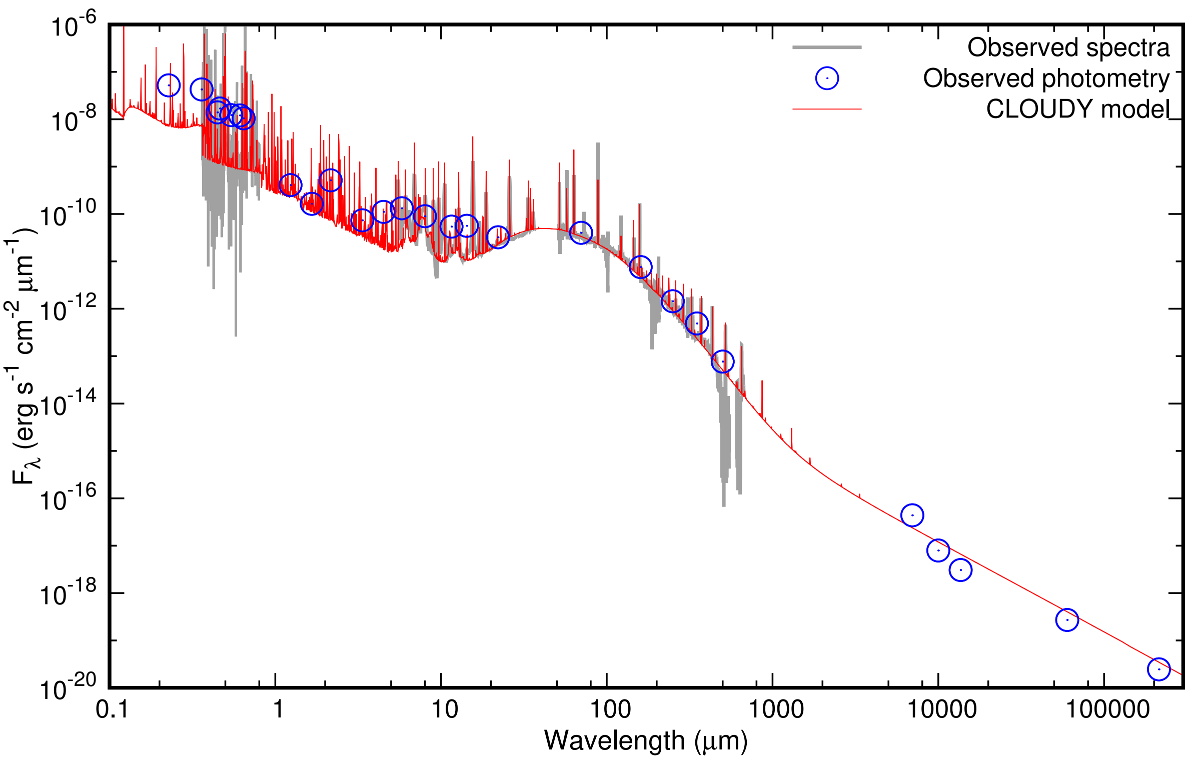

Figure 2. The full SED of the best-fit Cloudy model of NGC6781 (red line; spectral resolution R = 300), compared with the observational constraints: photometry data (blue circles) and spectroscopy data (grey line). The photometry data of central star listed in Table 1 and presented in Figure 2 are used to characterize the SED and determine the luminosity and distance (0.46 kpc) of the central star as the heating and ionising source; the effective temperature and luminosity of the central star are 120 870 K and 121 $L_{\odot}$ in the best fitting, respectively. This figure is taken from Otsuka et al. (2017).

region of the nebula. This finding emphasizes that while PNe are known as the hallmark of ionized gas in H^+ regions, the colder dusty PDR that surrounds the ionized gas carries greater significance in terms of the progenitor's mass-loss history and cannot be neglected to account for the full energetics of the nebula.

The present work has demonstrated that PNe can indeed serve as (1) empirical constraints for stellar evolutionary models, because empirically derived central star and nebula parameters can now comprehensively confront theoretical predictions (and the present AGB models are shown to be correct in general), and (2) important probes of mass recycling and chemical evolution in galaxies because PNe would permit one of the most thorough mass accounting of the mass-loss ejecta in the circumstellar environments. From our detailed multiwavelength analysis of NGC6781, we emphasise that characterizing PDRs and estimating warm-cold gas/dust masses in any astronomical objects would be very important for fully understanding stellar evolution and material recycling in galaxies. Dataset provided by Far-IR *AKARI*/FIS and *Herschel*/PACS/SPIRE have a critical role to investigate PDRs in PNe. A more detailed discussion is found in Otsuka et al. (2017).

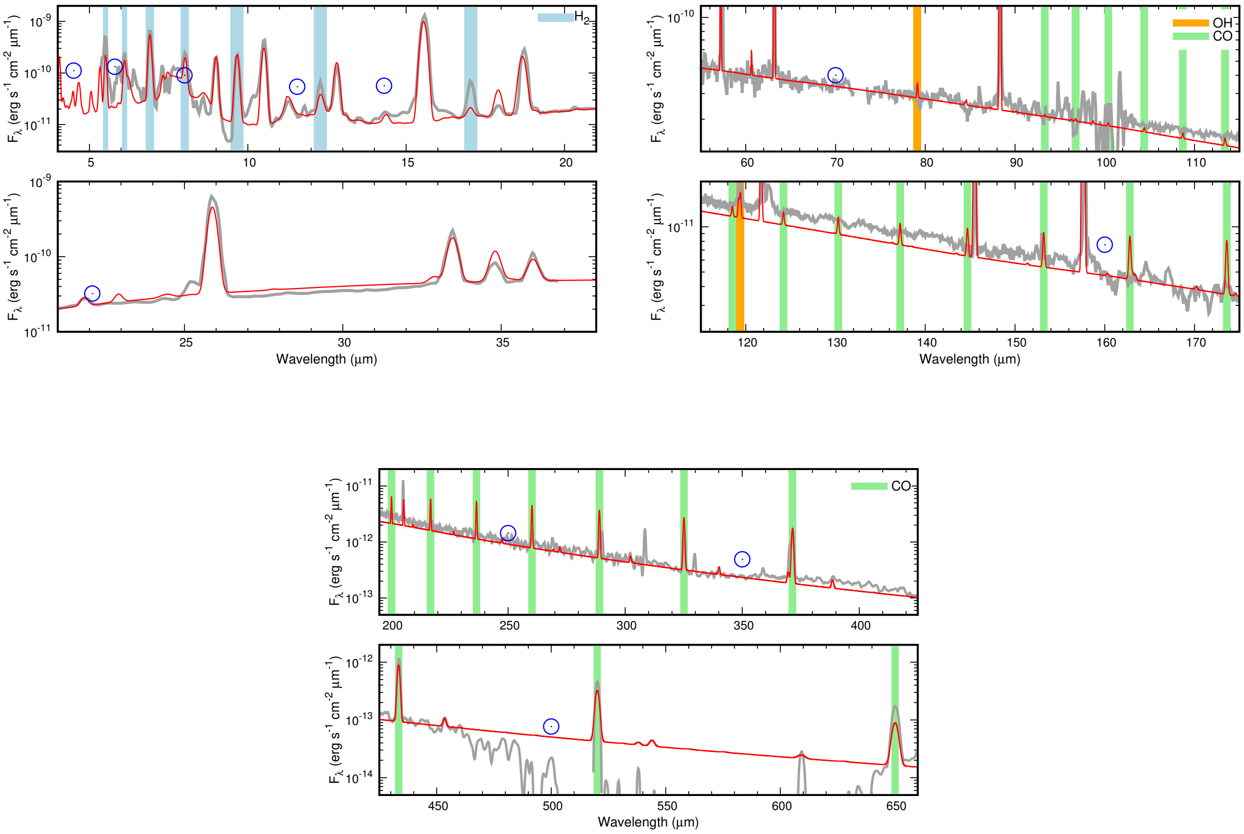

Figure 3. Comparison between the SED of the best-fit Cloudy model (red line, with undetectable atomic and molecular lines ($< 10^{-2}$ % of the Hβ line flux) removed; R = 100 in the top 2 frames and R = 480 in the bottom frame, corresponding to the resolution of the instrument in the respective bands) and the observational data (spectra in grey line and photometry in blue circles) in IR regions (top left: *Spitzer*/IRS; top right: *Herschel*/PACS; bottom: *Herschel*/SPIRE). The positions of molecular line emission are highlighted: rotational H_2 lines (light blue), OH (yellow), and ^{12}CO (light green). These figures are taken from Otsuka et al. (2017).

ACKNOWLEDGMENTS

MO was supported by the research fund 104-2811-M-001-138 and 104-2112-M-001-041-MY3 from the Ministry of Science and Technology (MOST), R.O.C. TU was partially supported by an award to the original *Herschel* observing program (OT1_tueta_2) under Research Support Agreement (RSA) 1428128 issued through JPL/Caltech, and by the NASA under Grant NNX15AF24G issued through the Science Mission Directorate.

REFERENCES

Condon, J. J., Cotton, W. D., Greisen, E. W., et al. 1998, AJ, 115, 1693
Ferland, G. J., Porter, R. L., van Hoof, P. A. M., et al. 2013, RMxAA, 49, 137
Flower, D. R., & Pineau Des Forêts, G. 2010, MNRAS, 406, 1745
Karakas, A. I. 2010, MNRAS, 403, 1413
Liu, Y., Liu, X.-W., Barlow, M. J., & Luo, S.-G. 2004a, MNRAS, 353, 1251
Liu, Y., Liu, X.-W., Luo, S.-G., & Barlow, M. J. 2004b, MNRAS, 353, 1231
Lodders, K. 2010, in Principles and Perspectives in Cosmochemistry, ed. A. Goswami & B. E. Reddy, 379
Otsuka, M., Ueta, T., van Hoof, P. A. M., et al. 2017, ApJS, 231, 22
Pazderska, B. M., Gawroński, M. P., Feiler, R., et al. 2009, A&A, 498, 463
Petrov, L., Hirota, T., Honma, M., et al. 2007, AJ, 133, 2487
Stanghellini, L., & Haywood, M. 2010, ApJ, 714, 1096
Ueta, T., Ladjal, D., Exter, K. M., et al. 2014, A&A, 565, A36
Umana, G., Leto, P., Trigilio, C., et al. 2008, A&A, 482, 529
van Hoof, P. A. M., van de Steene, G. C., Barlow, M. J., et al. 2010, A&A, 518, L137